Food and Chemical Toxicology 197 (2025) 115301

Contents lists available at ScienceDirect

Food and Chemical Toxicology

journal homepage: www.elsevier.com/locate/foodchemtox

Fraglide-1 from traditional Chinese aromatic vinegar: A natural AhR antagonist for atopic dermatitis

Kosuke Kato [a], Miki Akamatsu [b], Saya Kakimaru [a], Mayuko Koreishi [a], Masahiro Takagi [c], Masahiro Miyashita [d], Yoshiyuki Murata [b], Yoshimasa Nakamura [b], Ayano Satoh [a,*], Yoshio Tsujino [e,**]

[a] Graduate School of Interdisciplinary Science and Engineering in Health Systems, Okayama University, Okayama, 700-0082, Japan
[b] Graduate School of Environmental and Life Science, Okayama University, Okayama, 700-8530, Japan
[c] School of Materials Science, Japan Advanced Institute of Science and Technology, 1-1 Asahidai, Nomi, Ishikawa, 923-1292, Japan
[d] Graduate School of Agriculture, Kyoto University, Kitashirakawa-oiwake-cho, Sakyo-ku, Kyoto, 606-8502, Japan
[e] Graduate School of Science, Technology and Innovation, Kobe University, Kobe, 657-8501, Japan

ARTICLE INFO

Handling Editor: Dr. Bryan Delaney

Keywords:
AhR
Xenobiotic responsive element
StemRegenin 1
ARNT
Atopic dermatitis
Artemin

ABSTRACT

Traditional Chinese Zhenjiang aromatic vinegar (Kozu) contains Fraglide-1 (FG1), a bioactive lactone with demonstrated peroxisome proliferator-activated receptor gamma (PPARγ) agonist and antioxidant activities. This study explored FG1's novel ability to antagonize the aryl hydrocarbon receptor (AhR) signaling pathway, which regulates artemin expression and contributes to itching and inflammation in atopic dermatitis. Through molecular docking simulations and cell-based assays in human keratinocytes, we demonstrated FG1's potent antagonistic activity against AhR signaling. FG1 effectively suppressed FICZ-induced inflammatory responses, including artemin expression, with potency (half maximal inhibitory concentration, IC_{50} = 5.1 μM) comparable to the synthetic antagonist StemRegenin 1 (SR1) while demonstrating a superior safety profile (median lethal concentration, LC_{50} > 100 μM vs. 27.5 μM for SR1). These findings expand our understanding of bioactive compounds from traditional fermented foods and their regulatory effects on AhR signaling, providing a foundation for future studies on FG1's role in modulating skin inflammation.

1. Introduction

Fraglide-1 (5-hydroxy-4-phenyl-butenolide, FG1) is a bioactive lactone characterized by a four-carbon heterocyclic ring structure (Pubchem CID: 140781916). This compound was originally isolated from Kozu, a Chinese Zhenjiang aromatic vinegar (Yatmaz et al., 2017). Kozu, produced through the natural fermentation of glutinous rice followed by prolonged aging, represents a remarkable example of how traditional food processing can enhance the formation of beneficial compounds. This fermented condiment has been an integral part of Chinese cuisine and traditional medicine for millennia, valued for its potential to ameliorate lifestyle-related conditions. Our preclinical studies in mice [Patent: WO2016006548A1] demonstrated that FG1 exhibits anti-obesity effects through activation of peroxisome proliferator-activated receptor γ (PPARγ) (Tsujino, 2017), leading to improved glucose metabolism via enhanced fatty acid oxidation through mitochondrial uncoupling protein 1 (UCP1, also known as thermogenin) (Gong et al., 2024). Beyond its metabolic benefits, FG1 has shown promising antifungal (Koshino et al., 1992; Dickschat, 2017) and antioxidant properties, with the latter mediated through the nuclear factor

Abbreviations: AhR, aryl hydrocarbon receptor; ARE, antioxidant response element; ARNT, AhR nuclear translocator; CA, cinnamaldehyde; EC_{50}, Half maximal effective concentration; FG1, Fraglide-1; FICZ, 6-formylindolo(3,2-*b*)carbazole; HIF1α, hypoxia-inducible factor 1-alpha; HRE, hypoxia response element; I3C, indole-3-carbinol; IC_{50}, Half maximal inhibitory concentration; IND, indirubin; ITE, 2-(1′*H*-indole-3′-carbonyl)-thiazole-4-carboxylic acid methyl ester; Kozu, Chinese Zhenjiang aromatic vinegar; LC_{50}, Lethal concentration 50, median lethal concentration; LOAEL, The Lowest Observed Adverse Effect Level; Nrf2, nuclear factor erythroid 2-related factor 2; NOAEL, The No Observed Adverse Effect Level; PPARγ, peroxisome proliferator-activated receptor gamma; ROS, reactive oxygen species; SR1, StemRegenin 1; TSLP, thymic stromal lymphopoietin; VEGFA, vascular endothelial growth factor A; XRE, xenobiotic response element.

* Corresponding author.
** Corresponding author.
E-mail addresses: ayano113@cc.okayama-u.ac.jp (A. Satoh), ytsujino@tiger.kobe-u.ac.jp (Y. Tsujino).

https://doi.org/10.1016/j.fct.2025.115301
Received 14 December 2024; Received in revised form 27 January 2025; Accepted 29 January 2025
Available online 7 February 2025

erythroid 2-related factor 2 (Nrf2)/antioxidant response element (ARE) pathway (Tabei et al., 2017).

Like FG1, flavonoids are a class of compounds with considerable therapeutic potential in functional foods. These naturally occurring polyphenolic compounds are found in a wide variety of plant foods and beverages (Kaushal et al., 2022). In addition to their dietary ubiquity, flavonoids share similarities with FG1, including their structures and their functionalities in modulating key cellular pathways such as PPARγ (Zhang et al., 2019) and Nrf2 (Huang et al., 2023). Recent studies have shown that flavonoids exhibit diverse biological activities beneficial to human health, including anti-inflammatory and anticancer effects. Compounds such as quercetin and epicatechin have demonstrated roles in inhibiting cancer cell proliferation (Aghababaei and Hadidi, 2023) and providing cardiovascular benefits (Ciumărnean et al., 2020). Recent studies have also identified flavonoids as AhR ligands (Goya-Jorge et al., 2021).

AhR is a ligand-activated transcription factor that can be modulated by both dietary intake and direct exposure to bioactive compounds (Mo et al., 2020). While many food-derived compounds like FG1 show promising biological activities, their effectiveness can be limited by bioavailability and tissue distribution when consumed orally. However, AhR's abundant expression in epidermal keratinocytes presents an opportunity for direct topical application of these compounds, potentially achieving higher local concentrations at the target site. Upon encountering an agonist, AhR is activated and translocates to the nucleus, where it forms a heterodimer with the AhR nuclear translocator (ARNT). This complex then binds to xenobiotic response elements (XRE) in the promoter regions of target genes. Recent studies have revealed that AhR plays a pivotal role in epidermal homeostasis and barrier function, particularly in the context of atopic dermatitis, by regulating the expression of artemin under its control (Hidaka et al., 2017; Edamitsu et al., 2019). Abnormal expression of artemin, driven by AhR signaling, leads to the aberrant extension of neurons toward the skin surface, contributing to the pathogenesis of atopic dermatitis. In atopic dermatitis lesions, this abnormal neuronal extension results in itching sensations, further exacerbating the condition. Currently, evaluation of potential therapeutic agents for atopic dermatitis typically requires animal models such as NC/Nga mutant mice (Matsuda et al., 1997), but cell-based systems that can assess AhR modulation and artemin expression could provide an alternative approach with the 3Rs consideration.

Given these opportunities, we sought to investigate the potential of FG1 as an AhR ligand. We began our investigation with docking simulations to evaluate the interaction between FG1 and the AhR binding pocket, using the known interaction of apigenin, a well-characterized food-derived flavonoid, as a reference. Encouraged by these simulation results, we established a cell-based assay using a human skin keratinocyte cell line to measure the effects of FG1 on AhR-regulated gene expression, particularly artemin. Furthermore, we compared FG1's efficacy and safety with known AhR antagonists including StemRegenin 1 (SR1). Our findings provide new insights into how FG1, a compound originally isolated from aromatic vinegar, regulates AhR signaling and could inform future studies on its role in managing atopic dermatitis through dietary supplementation or topical application, adding to its known anti-obesity, antifungal, and antioxidant effects.

2. Methods

2.1. Human AhR protein–ligand docking simulations

Molecular modelling and docking simulations were performed using the molecular modelling and simulation programme YASARA ver. 23.5.19 (YASARA Biosciences GmbH; Vienna, Austria, Krieger and Vriend, 2014). Residues Pro271 through Leu427 of the human AhR protein (PDB: 7ZUB, chain D) were extracted and used as the binding domain for docking. The 3D structures of apigenin, quercetin and FG1-1 were obtained from PubChem (PubChem CID: 5280443, 5280343 and 12864804, respectively). The other FG1 structure (FG1-2) was modified from that of FG1-1 (Supplementary Fig. S1). All the compound structures were then energy minimized by the YASARA2 force field.

Ensemble docking simulations of apigenin, quercetin, and FG1 (FG1-1 and FG1-2) to the AhR-binding domain were performed. Ensemble docking involves docking a ligand to a receptor ensemble with flexible side chains. All residues within 5.0 Å of the original ligand in the PDB 7ZUB protein binding pocket were selected for the docking site. AutoDock VINA (Trott and Olson, 2010, Eberhardt et al., 2021) was applied for YASARA ensemble docking, and the default settings were used for all calculations. The 20 ligand poses for each of the five receptors in the ensemble (for a total of 100 poses) were obtained, and the binding energy of the poses was calculated using the AMBER03 force field. The docking pose with the maximum binding energy for each ligand was selected. The known AhR agonists/antagonists apigenin and quercetin aligned well in the simulation, confirming that the optimization of the simulation was successful.

2.2. Reporter cell line for AhR-dependent transcription

The method for establishing the stable cell line has been previously described in detail (Selvam et al., 2020; Liu et al., 2022). In summary, HaCaT cells obtained from the German Cancer Research Center (DKFZ, Heidelberg, Germany) were cultured in Dulbecco's modified Eagle's medium supplemented with 10% foetal bovine serum. These cells were transfected with pNL[NlucP/XRE/Hygro] (#CS186808; Promega Japan, Tokyo, Japan). After transfection, cells that consistently expressed the transgene were selected using hygromycin. The resulting cell line was referred to as "XRE-NLuc:HaCaT".

2.3. Reporter assays and cell viability measurements

Assays were performed as described previously (Sato et al., 2024). In brief, XRE-NLuc:HaCaT cells were seeded in a white 96-well plate with 10,000 cells in 100 μl per well. After 24 h of culture, the culture supernatants were discarded. The cells were then treated with the test compounds diluted in culture medium and incubated for an additional 23 h. Three microlitres of WST-1 assay reagent (#MK400; Takara Bio, Shiga, Japan) was added, and the mixture was incubated for 1 h. The culture supernatants were then transferred to a transparent 96-well plate, and absorbance was measured at 450 nm with a reference wavelength of 670 nm (A450-A670) using a microplate reader (iMark; Bio-Rad Japan, Tokyo, Japan) to determine cell viability. To the cells remaining in the white wells of the plate, 10 μl of NLuc substrate (#N1120, Promega) was added. After incubation for 5 min, the resulting luminescence was read using a GloMax® Navigator Microplate Luminometer (Promega). The luminescence, which indicates reporter expression, was then normalized relative to the absorbance-derived number of viable cells. In this study, a cell viability less than 70% was considered toxic.

The following agents were used for evaluation in this study, as summarized in Supplementary Table S1. FG1 (Fraglide-1, 5-hydroxy-4-phenyl-butenolide) was prepared in-house with a purity of >97%. FICZ (6-Formylindolo[3,2-*b*]carbazole) was obtained from ChemScene-Funakoshi (catalog #CS-3513, Tokyo, Japan) with >99% purity. CA (*trans*-cinnamaldehyde) was sourced from Nacalai (catalog #09024-72, Kyoto, Japan) at a purity of ≥98%. I3C (indole-3-carbinol) was purchased from LKT LABS-Funakoshi (catalog #I5213) with ≥98% purity. SR1 (StemRegenin 1) was acquired from ChemScene-Funakoshi (catalog #CS-1643) at a purity of ≥99%. Resveratrol was obtained from FUJIFILM (catalog #185–01721, Osaka, Japan) with ≥98% purity. ITE (2-(1′*H*-indole-3′-carbonyl)-thiazole-4-carboxylic acid methyl ester) was purchased from TOCRIS-Funakoshi (catalog #1803, Tokyo, Japan) with a purity of ≥99%. IND (indirubin) was sourced from Toronto Research Chemicals-Funakoshi (catalog #I521350, Toyo, Japan) with ≥95%

purity. Glycerol was obtained from FUJIFILM (catalog #070–04941) at ≥99% purity, and DMSO (dimethyl sulfoxide) was purchased from Nacalai (catalog #09659-14) with a purity of ≥99.5%.

To determine the relative cell viability, we used the following equation: Relative cell viability = [(A450 of cells exposed to test compound) - (A670 of cells exposed to test compound)]/[(A450 of cells exposed to vehicle) - (A670 of cells exposed to vehicle)]. For fold induction calculations, the formula was adapted to utilize luminescence values in lieu of absorbance readings. The median lethal concentration at which 50% of the cells were affected (LC_{50}) was calculated using the following equation: $LogLC_{50} = [(50 - c) \times Log(b) - (50 - a) \times Log(d)]/(a - c)$, where a is the minimum viability at which the cell viability is >50%, c is the maximum viability at which the cell viability is <50%, and b and d are the concentrations at which the cell viability is assessed. Both the IC_{50} (the concentration of a compound at which 50% of its maximal inhibitory effect is observed) and the EC_{50} (the concentration of a compound at which 50% of its maximal effect is observed) were calculated using the LC_{50} formula but replacing the viability with fold induction values. To determine the maximum induction, we plotted the fold induction against the respective concentrations. The data were then subjected to curve fitting using an Excel plot chosen based on its fit to our dataset. The point at which the maximum induction occurred on the fitted curve was identified to estimate the corresponding concentration.

2.4. cDNA preparation and qPCR

cDNA preparation and qPCR were performed as described previously (Kyunai et al., 2023). Briefly, total RNA was extracted and reverse transcribed using a SuperPrep II Cell Lysis & RT Kit for qPCR (#SCQ-401; Toyobo, Tokyo, Japan) according to the manufacturer's instructions. The obtained cDNA was subjected to quantitative polymerase chain reaction (qPCR) with THUNDERBIRD Next SYBR qPCR Mix (#QPX-201, Toyobo) according to the manufacturer's protocol using the StepOne Real-Time PCR System (Thermo Fisher Japan, Tokyo, Japan). The expression of each gene obtained by qPCR was normalized to that of GAPDH. The primer sets used in this study are listed in Supplementary Table S2.

2.5. Sodium dodecyl sulfate–polyacrylamide gel electrophoresis and western blotting

Sodium dodecyl sulfate–polyacrylamide gel electrophoresis (SDS–PAGE) and western blotting were performed as described previously (Sato et al., 2024). Cell lysates were prepared in lysis buffer (10 mM HEPES-KOH, pH 7.4; 100 mM KCl; 1 mM MgCl2; 1% Triton X-100; and protease inhibitor cocktails (Nacalai, Kyoto, Japan)). After incubation for 10 min on ice, the lysate was clarified by centrifugation at 14, 000×*g* for 10 min. The supernatants were then subjected to SDS–PAGE on a 7.5% gel (Bio-Rad, Hercules, CA, USA). The proteins were electrotransferred to polyvinylidene fluoride or polyvinylidene difluoride membranes (pore size: 0.45 μm; Merck Group Japan, Tokyo, Japan). The proteins on the membrane were detected by incubation with diluted anti-ARNT (Santa Cruz Biotechnology, Cosmo Bio Co., Ltd., Tokyo, Japan) and anti-γ-tubulin (Sigma, Sigma–Aldrich Japan, Tokyo, Japan) antibodies followed by incubation with HRP-conjugated anti-mouse immunoglobulin G (Cell Signaling Technology, CST Japan, Tokyo, Japan) using a charge-coupled device camera.

2.6. Statistical analysis

The data were analyzed using Student's t-test for independent samples. A *P* value less than 0.05 was considered to indicate statistical significance. LOAEL and NOAEL values were determined from dose-response data by identifying the lowest concentration at which statistically significant effects were observed (LOAEL) or no significant effects were detected (NOAEL) compared to the control. All analyses were performed with Microsoft Excel for Mac (version 16).

3. Results

3.1. Docking simulations revealed that the natural compound FG1 interacts with AhR similarly to flavonoids

To understand how this vinegar-derived bioactive compound might interact with its molecular target, we first compared FG1's structure with those of well-known food-derived AhR ligands. Given the structural similarities between dietary flavonoids and FG1, we performed docking simulations of the flavonoids quercetin and apigenin, the latter being a well-characterized AhR ligand (Jin et al., 2018), and two stereoisomers of FG1 (FG1-1 and FG1-2) with AhR (Supplementary Fig. S1). FG1 exists as stereoisomers, but their relative abundances in natural sources, such as vinegar, are not yet known. As shown in Fig. 1a, common dietary flavonoids quercetin (gray) and apigenin (magenta) exhibited similar docking patterns to AhR, forming π-π and CH-π interactions with His291, Phe295, Pro297, Phe 324, Ile325, Phe351, and Leu353. Notably, the docking pose of FG1-1 (orange, Fig. 1b) was similar to that of apigenin. This alignment of FG1-1 with apigenin (magenta, Fig. 1b) suggested that FG1 could modulate the AhR signaling pathway in a manner similar to these dietary flavonoids. Fig. 1c shows the alignment of the docking poses of FG1-1 (orange) and FG1-2 (purple). Although FG1-2 binds to AhR in a different mode than does FG1-1, the phenyl groups of both isomers occupy the same area in the binding pocket, suggesting that each of these two groups may affect the function of AhR.

3.2. FICZ induces artemin expression in epidermal cells

To validate the effects of FICZ, a known AhR agonist, on atopic dermatitis-related gene expression, we performed qPCR to determine if it would induce mRNA expression of artemin and thymic stromal lymphopoietin (TSLP), both of which are found in atopic dermatitis lesions (Hidaka et al., 2017; Edamitsu et al., 2019). As expected, FICZ dose-dependently increased the mRNA levels of these genes (Fig. 2a and b), supporting the use of AhR agonist-treated cells as a model for atopic dermatitis-like conditions. The qPCR data shown in Fig. 2a is also supported by our published RNA sequencing data (BioProject: PRJDB17333). These results confirm previous findings that artemin upregulation is mediated by AhR agonists (Hidaka et al., 2017; Edamitsu et al., 2019) and indicate that monitoring AhR activation or inhibition can reflect changes in artemin expression in this system.

3.3. Development and validation of a cell-based assay system for AhR modulation

Having established that FICZ induces expression of atopic dermatitis-related genes, we sought to develop a quantitative system to screen for compounds that could modulate AhR activity. To determine the potential effect of natural compounds, including FG1, on AhR-dependent transcription, we established a HaCaT human keratinocyte cell line stably exp.ressing NanoLuc luciferase under three XRE motifs (CACGC) (Fig. 3a: vector map; Fig. 3b: cell image, Bak et al., 2017). The stable integration of the reporter construct into the genome allows for consistent expression of the transgene, providing an advantage over transient transfection systems.

We first validated this cellular assay system using established AhR agonists such as 6-formylindolo(3,2-*b*), carbazole (FICZ), indirubin (IND), 2-(1′*H*-indole-3′-carbonyl)-thiazole-4-carboxylic acid methyl ester (ITE), and indole-3-carbinol (I3C) (Hubbard et al., 2015). The tryptophan derivative FICZ, an endogenous AhR agonist (Rannug and Rannug, 2018), showed a dose-dependent response with peak induction noted at 500 nM and an EC_{50} of 12 nM (Fig. 3c). Fig. 3d presents the corresponding effects on cell viability. Validation extended to other endogenous AhR ligands, including IND, and dietary metabolites like

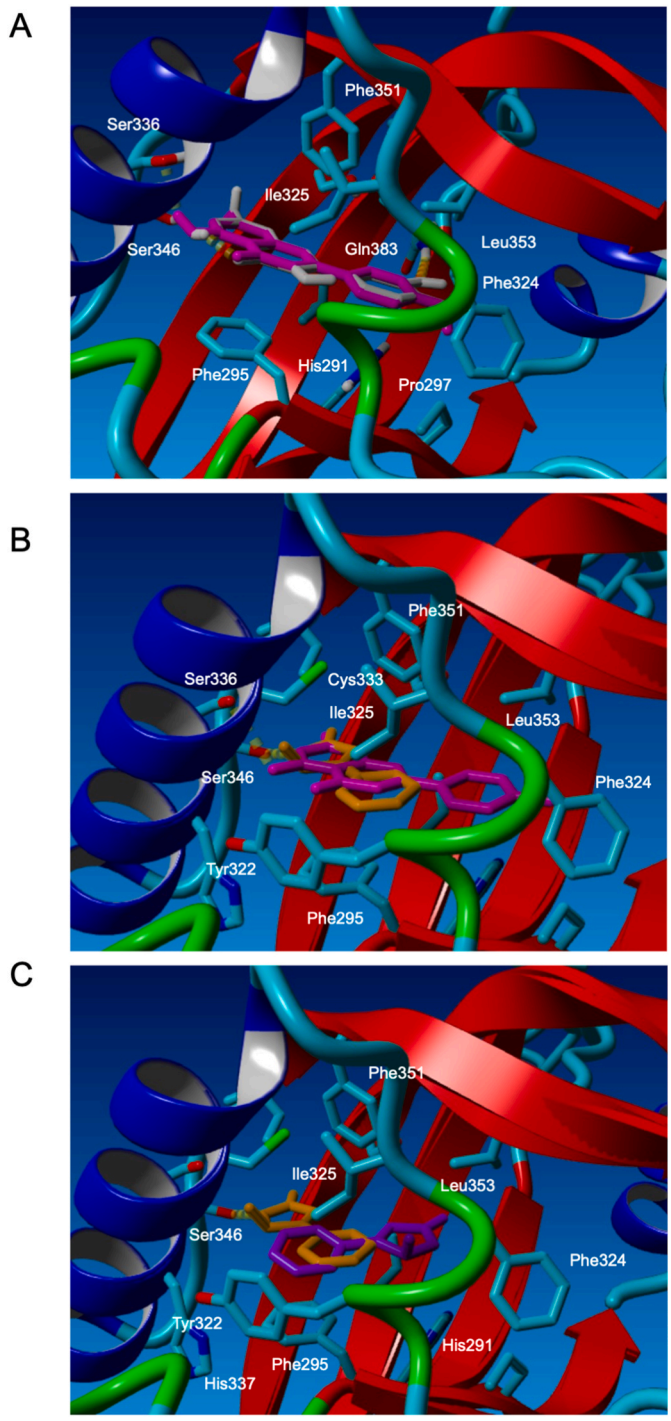

Fig. 1. Molecular docking analysis of FG1 and flavonoids with AhR
Docking simulations of quercetin, apigenin and FG1 to the AhR-binding domain (PDB ID: 7ZUB, chain D) were performed using YASARA. The 3D structures of quercetin, apigenin and FG1-1 were obtained from PubChem (CID 5280343, 5280443 and 12864804, respectively), and all energies were minimized using the YASARA2 force field. The docking pose with the maximum binding energy calculated using the AMBER03 force field for each ligand was selected. (a) Alignment of quercetin (gray) and apigenin (magenta) docked to the AhR-binding domain. (b) Alignment of the docking patterns of FG1 (orange) and apigenin (magenta) to the AhR-binding domain. (c) Alignment of the docking positions of the FG1 stereoisomers FG1-1 (orange) and FG1-2 (purple) to the AhR-binding domain. (For interpretation of the references to colour in this figure legend, the reader is referred to the Web version of this article.)

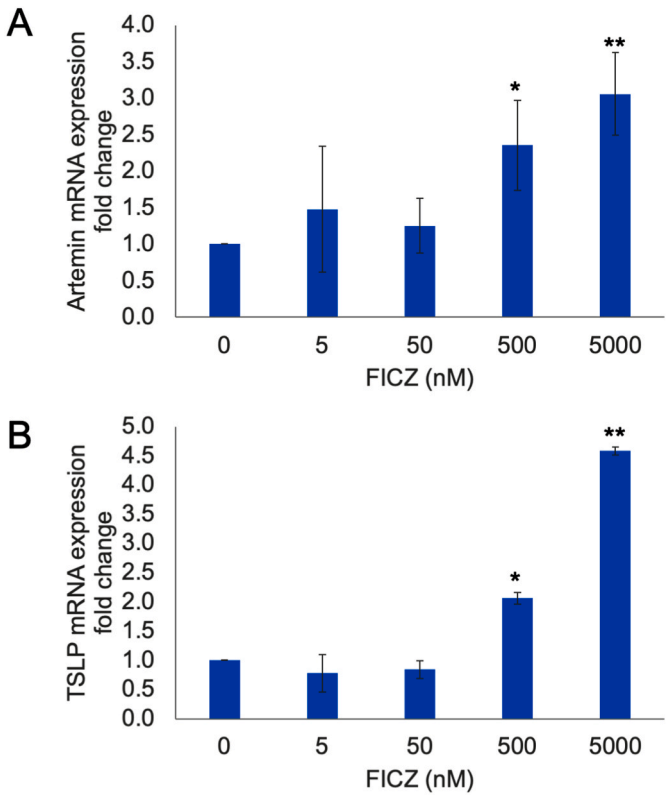

Fig. 2. FICZ induces inflammation-related genes in epidermal cells
(a, b) Expression of inflammation-related genes, artemin and TSLP mRNA, after FICZ treatment. Cells were exposed to indicated concentrations of FICZ for 24 h. Results are expressed as fold changes relative to vehicle control. Error bars indicate standard deviations (SDs; n = 2–4). $^{*}P < 0.05$, $^{**}P < 0.01$ vs vehicle control (Student's t-test).

ITE and I3C, further confirming the system's robustness. Table 1 summarizes the respective EC_{50} and LC_{50} values calculated from the data shown in Supplementary Fig. S2. Comparison of our results with external studies revealed consistent responses to these recognized AhR agonists (Rannug and Rannug, 2018; Adachi et al., 2001; Hubbard et al., 2015; Song et al., 2002; Aggarwal and Ichikawa, 2005). This consistency confirms the assay's reliability and reproducibility for screening AhR modulators. Glycerol, used as a negative control, showed no induction of reporter expression, confirming the specificity of our assay system for AhR-mediated responses.

Having validated our reporter system with agonists, we next evaluated the effects of known AhR antagonists including StemRegenin 1 (SR1) (Boitano et al., 2010), cinnamaldehyde (CA) (Uchi et al., 2017), and resveratrol (Casper et al., 1999; Revel et al., 2003). The vehicle control (DMSO) was set as the reference value (1.0) for relative luciferase activity. As shown in Fig. 4a–d, these AhR antagonists suppressed reporter expression in a dose-dependent manner. Table 2 summarizes the 50% inhibitory concentration (IC_{50}) values calculated from Fig. 4a–d and LC_{50} values from Supplementary Fig. S2. Using the same assay conditions, we found that FG1 suppressed reporter activity in a dose-dependent manner, with an IC_{50} of 5.1 μM. Notably, FG1 exhibited similar potency to SR1 but demonstrated a substantially improved safety profile, with an LC_{50} value > 100 μM compared to SR1's LC_{50} of 27.5 μM (Table 2).

The lowest observed adverse effect level (LOAEL) for FG1 was identified as 1.56 μM, the same as SR1, based on its significant suppression of AhR reporter activity (Fig. 4a–d). For cell viability, FG1's no observed adverse effect level (NOAEL) was determined to be 100 μM, significantly higher than SR1's NOAEL of 6.25 μM, as shown in Supplementary Fig. S2. These results demonstrate that FG1 is as potent as

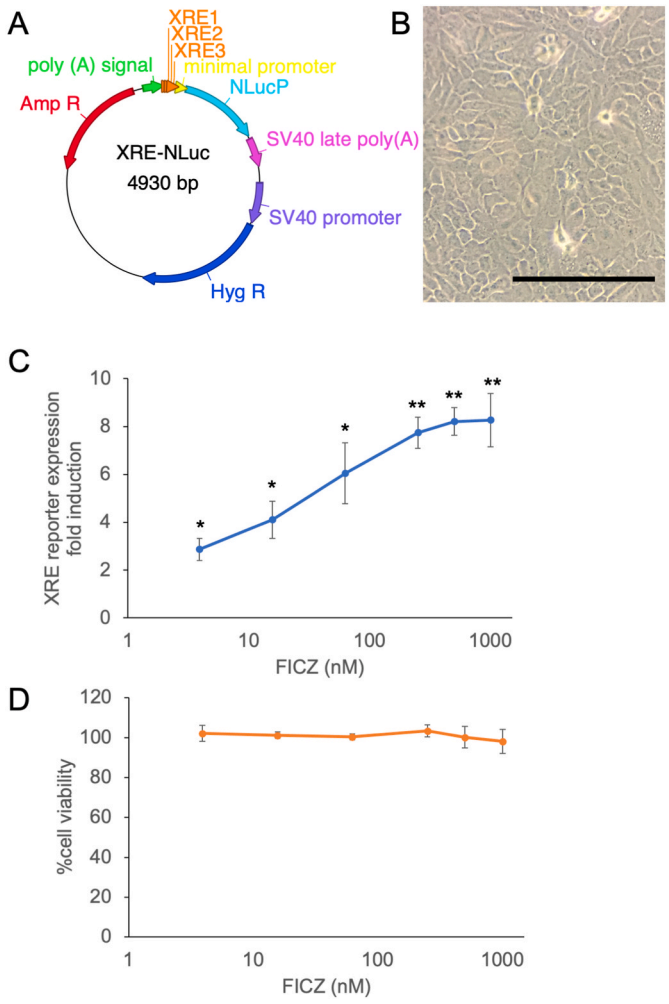

Fig. 3. Validation of reporter cells for AhR-dependent transcription
The human keratinocyte cell line HaCaT was stably transformed to express the NanoLuc reporter gene (NLucP) driven by three artificially introduced XRE sequences (XRE1, XRE2, and XRE3) and a minimal promoter. (a) Vector map. The vector contains NanoLuc reporter gene (NLucP) under the control of three XRE sequences and a minimal promoter, along with hygromycin resistance gene (Hyg R) for selection. (b) XRE-NLuc:HaCaT cells. Scale bar, 250 μm. (c) Response to the AhR agonist FICZ. Cells were treated with indicated concentrations of FICZ for 24 h. Data are expressed as fold changes in reporter expression relative to vehicle control. Error bars represent SEMs (n = 4, biological triplicates). *P < 0.05, **P < 0.01 compared with vehicle. (d) Cell viability under the same conditions. Error bars represent SEMs (n = 4).

SR1 in modulating AhR signaling but exhibits a much safer profile.

3.4. FG1 effectively suppresses FICZ-induced AhR signaling in a cellular model of skin inflammation

Following our validation of the reporter system, we next investigated FG1's potential to modulate AhR signaling in a disease-relevant context. Given that genes associated with the onset and exacerbation of atopic dermatitis are regulated by AhR (Hidaka et al., 2017; Edamitsu et al., 2019), we developed a cellular model where exposure to the AhR agonist FICZ could mimic inflammatory skin conditions. To test potential modulators, XRE-NLuc:HaCaT cells were treated with FICZ in combination with FG1, SR1 (Boitano et al., 2010) or CA (Uchi et al., 2017) to evaluate their antagonistic effects. The data are presented as percent inhibition, where 0% represents the FICZ-induced response without antagonist, and 100% represents complete suppression of FICZ effects.

Table 1
AhR agonists used in this study.

	#CAS	Maximum induction (μM)		EC_{50} (μM)	LC_{50} (μM)
		literature[a,b]	this study	this study	this study
FICZ (6-Formylindolo [3,2-*b*]carbazole)	172922-91-7	1[b]	0.5	0.012	>1
I3C (indole-3-carbinol)	700-06-1	–	175	11	>700
ITE (2-(1′*H*-indole-3′-carbonyl)-thiazole-4-carboxylic acid methyl ester)	448906-42-1	10[b]	25	1.3	>100
IND (Indirubin)	479-41-4	5~10[a]	0.25	0.0006	>1

[a] (Novotna et al., 2011).
[b] (Satsu et al., 2015).

As shown in Fig. 4e, both FG1 and SR1 showed potent antagonism of FICZ-induced reporter expression, with IC_{50} values of approximately 6.7 and 5.2 μM, respectively. These values were slightly different from the IC50 values obtained without FICZ induction (1.6 and 5.1 μM, respectively), as shown in Table 2 and Fig. 4a–d, but remained comparable. In contrast, CA showed limited antagonistic effects, with maximal inhibition not exceeding 50% under the tested conditions. Consistent with earlier results, FG1 maintained cell viability with an LC_{50} of over 100 μM, while SR1's LC_{50} was approximately 27.5 μM (Supplementary Fig. S2 and data not shown).

To further validate FG1's effects, we evaluated its ability to suppress FICZ-induced artemin expression, a key factor in atopic dermatitis pathogenesis. Fig. 4f shows the percent inhibition of FICZ-induced artemin expression by FG1, where 0% indicates no inhibition (full FICZ response) and 100% represents complete suppression of the FICZ effect. FG1 showed dose-dependent inhibition, with 0.1 μM FG1 achieving approximately 50% inhibition and 1 μM FG1 reaching nearly complete suppression. This finding is consistent with the observation that artemin is minimally expressed in typical keratinocytes. Thus, FG1 restored the expression level of artemin to its natural state in a dose-dependent manner, demonstrating FG1's potential for modulating artemin expression in skin conditions characterized by its abnormal regulation.

3.5. FG1 modulates ARNT levels to regulate AhR signaling

To further elucidate the molecular basis of FG1's modulatory effects, we investigated the mechanisms underlying its antagonism of AhR signaling. The AhR signaling cascade begins when AhR translocates to the nucleus upon binding to its agonist. In the nucleus, AhR forms a heterodimer with ARNT, which then binds to XRE to activate downstream gene expression. ARNT availability is a critical factor in this process, as it serves as a cofactor not only for AhR but also for other transcriptional pathways. Furthermore, the AhR repressor (AhRR) can compete with AhR for ARNT binding, inhibiting AhR-dependent transcription (Mimura et al., 1999).

Given ARNT's essential role in AhR signaling, we examined whether FG1 modulates ARNT and AhRR levels to alter transcription. As shown in Fig. 5a, FG1 dose-dependently increased AhR mRNA levels while decreasing ARNT mRNA levels. FG1 had no discernible effect on AhRR expression. These findings are supported by our published RNA sequencing data (BioProject: PRJDB13927). At the protein level, western blot analysis confirmed that FG1 treatment reduced ARNT levels in a dose-dependent manner, with approximately a 50% decrease observed (Fig. 5b). These results suggest that FG1 modulates AhR signaling by reducing ARNT levels, potentially limiting its availability for AhR-mediated transcription.

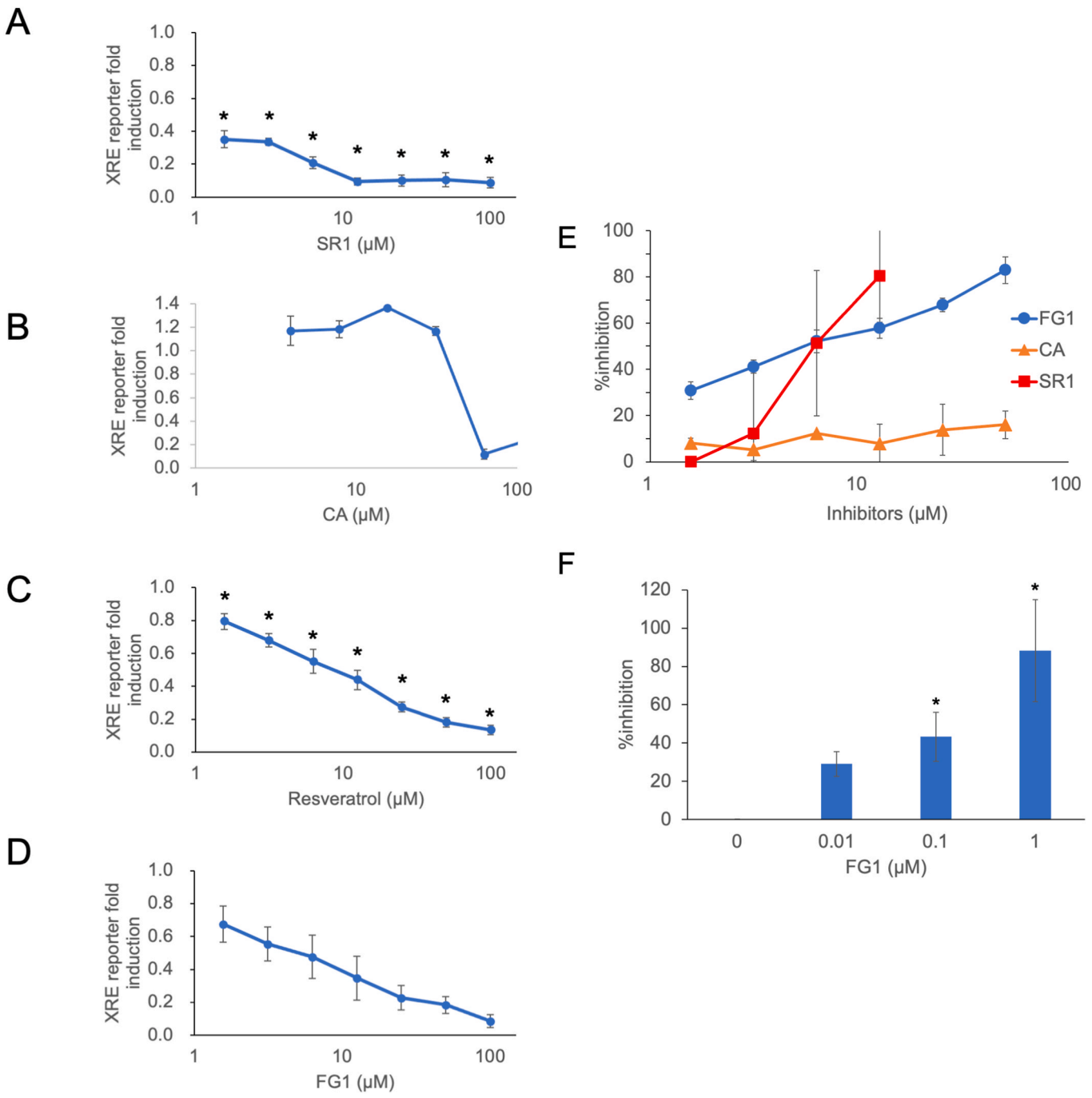

Fig. 4. FG1 demonstrates AhR antagonism and suppresses FICZ-induced effects
(a-d) Cells were treated with the indicated concentrations of SR1, CA, resveratrol, or FG1 for 24 h. Data are expressed as fold changes in reporter expression relative to the vehicle control. Values below 1.0 indicate suppression of basal reporter expression. Error bars represent SEM (n = 4 independent experiments, biological triplicates). *$P < 0.05$ vs. no drug (in a and d only). (e) Cells were treated with 5 μM FICZ together with the indicated concentrations of FG1 (circles), CA (triangles), or SR1 (squares) for 24 h. Data represent the percent inhibition of FICZ-induced reporter expression. Error bars represent SEM (n = 3). (f) Effects of FG1 on artemin expression determined by qPCR. Cells were treated with 5 μM FICZ and the indicated concentrations of FG1 for 24 h. Data represent the percent inhibition of FICZ-induced artemin expression. Error bars indicate SD (n = 3). *$P < 0.05$ vs. no FG1.

4. Discussion

In this study, we investigated the potential of FG1, a natural compound from traditional fermented vinegar. While FG1 was initially identified in Zhenjiang aromatic vinegar, quantitative analysis has confirmed its presence across various traditional Asian rice vinegars (Yatmaz et al., 2017), suggesting broader relevance as a bioactive compound in fermented rice products. Our investigation was guided by structural similarities between FG1 and dietary flavonoids, which can act as AhR agonists or antagonists depending on the cellular context (Goya-Jorge et al., 2021). Through molecular docking simulations, we demonstrated that FG1 binds to AhR in a manner similar to apigenin, a well-characterized dietary flavonoid. Using our NanoLuc reporter system in keratinocytes, we validated FG1's potent antagonistic activity, showing comparable potency to known AhR antagonists but with a superior safety profile. In a cellular model of skin inflammation, where the

Table 2
AhR antagonists used in this study.

	#CAS	IC_{50} (μM)		LC_{50} (μM)
		literature[a,b,c]	this study	this study
FG1 (Fraglide-1, 5H4PB)	**78920–11–3**	**-**	**5.1**	**>1000**
CA (*trans*-cinnnamaldehyde)	**104–55–2**	**~22[a]**	**48.5**	**55.8**
SR1 (StemRegenin 1)	**1227633–49–9**	**0.127[b]**	**1.6**	**27.5**
Resveraorol	**501–36–0**	**6[c]**	**8.5**	**>100**

[a] (Uchi et al., 2017).
[b] (Boitano et al., 2010).
[c] (Cheng et al., 2023).

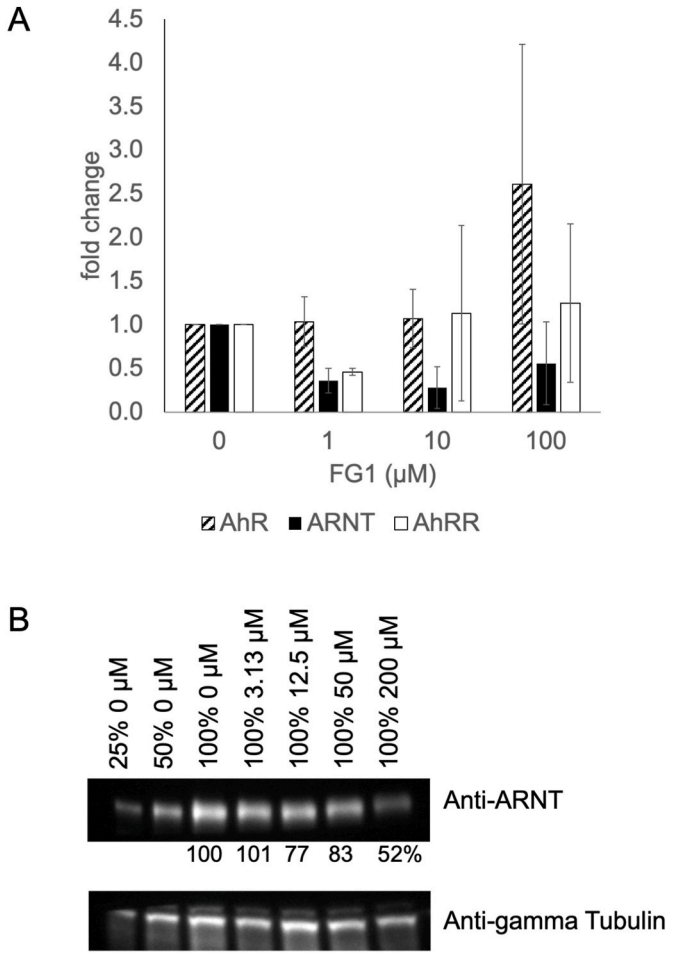

Fig. 5. Effects of FG1 on AhR signaling components
(a) Expression of AhR, ARNT, and AhRR mRNA levels determined by qPCR. Cells were treated with the indicated concentrations of FG1 for 24 h. Data are expressed as fold changes relative to the untreated control. Error bars represent standard deviations (SDs; n = 2–3). (b) (b) ARNT protein levels after FG1 treatment. Cell lysates were analyzed by western blotting using the indicated antibodies. γ-Tubulin served as a loading control. Values below the blot represent ARNT levels normalized to γ-tubulin, expressed as a percentage of the untreated control.

AhR agonist FICZ was used to mimic atopic dermatitis conditions, FG1 effectively suppressed artemin expression in a dose-dependent manner (Fig. 4f). At the molecular level, we discovered that FG1 modulates AhR signaling through ARNT attenuation, supported by decreases in ARNT mRNA and protein levels (Fig. 5a and b).

The comparisons of LOAEL and NOAEL comfirm FG1's safety margin. While FG1 and SR1 shared the same LOAEL for AhR inhibitory effects (1.56 μM, Fig. 4a–d), FG1 exhibited a significantly higher NOAEL for cell viability (100 μM vs. 6.25 μM for SR1, Supplementary Fig. S2). These findings indicate a broader therapeutic window for FG1 and a lower risk of adverse effects at higher concentrations, reinforcing its improved safety profile compared to SR1.

Structure-based searches revealed compounds with similar lactone scaffolds exhibiting diverse bioactivities. For example, Ganomycin I (PubChem CID: 46186831), isolated from mushrooms, shares structural features with FG1 and demonstrates inhibitory effects on α-glucosidase, HMG-CoA reductase, and HIV protease, along with anti-diabetic and anti-osteoclastogenesis properties. Another structurally related compound (CID: 44390691) inhibits nitric oxide synthesis. These findings suggest lactone-containing natural products may have broad therapeutic potential through multiple molecular targets.

Beyond its effects on AhR, FG1 was initially identified as a PPARγ agonist. PPARγ is predominantly expressed in adipocytes, where it plays a key role in regulating growth, functionality, and senescence. Recent evidence suggests that AhR modulates PPARγ protein stability through its function as a substrate receptor for the CUL4B-RING E3 ubiquitin ligase (CRL4B) complex, which marks target proteins, including PPARγ, for proteasomal degradation (Dou et al., 2019; Torti et al., 2021). These dual functions of AhR—transcriptional regulation and protein degradation—may be reciprocally regulated. In our HaCaT cell model, however, PPARγ did not respond to FG1 treatment (Supplementary Fig. S3), despite increased AhR expression (Fig. 5a) and enhanced overall ubiquitination (Supplementary Fig. S4). These findings suggest that FG1's effects on PPARγ may depend on tissue or cell type, with cellular context playing a critical role in modulating these pathways.

Following the identification of FG1 as a PPARγ agonist, its antioxidant properties were reported as another key bioactivity (Tabei et al., 2017). In addition to its role in mitigating oxidative stress, Nrf2 activation has been shown to increase hypoxia-inducible factor 1-alpha (HIF1α) expression and activity, influencing hypoxia-related pathways (Haddad et al., 2000; Luo et al., 2022). Interestingly, FG1 induced expression of HIF1α and vascular endothelial growth factor A (VEGFA), a gene regulated by hypoxia response elements (HREs) (Supplementary Fig. S5), suggesting that FG1 activates HRE-regulated genes through HIF1α. Given that both HIF1α and AhR signaling require ARNT as a cofactor, the activation of HIF1α by FG1 may antagonize AhR by sequestering ARNT. FG1-induced increases in HIF1α and VEGFA suggest a mechanism involving the interconnected roles of ARNT in both HRE- and XRE-mediated transcription. FG1 may modulate ARNT availability, altering the balance between AhR signaling and HIF1α-driven pathways.

While this study provides novel insights into FG1's role as an AhR antagonist and its potential mechanisms, several limitations warrant further investigation. First, the experiments were conducted primarily in the HaCaT cell line, which, although widely used in skin research, may not fully capture the complexity of atopic dermatitis pathogenesis. Additional studies using more physiologically relevant systems, such as 3D skin models or primary keratinocyte cultures, are needed to validate FG1's effects in more clinically relevant contexts.

Second, while docking simulations provided valuable insights into FG1's interaction with the AhR binding pocket, they represent a static view and may not fully account for the dynamic nature of ligand binding. Further experimental validation, including binding assays, time kinetics, and competition studies, will be essential to confirm these interactions. The establishment of AhR-deficient or modified HaCaT cells could also offer a more direct approach to evaluate FG1's specific effects on AhR signaling. However, multiple attempts to generate such cell lines were unsuccessful, possibly due to the essential role of AhR in keratinocyte homeostasis.

Third, while FG1's in vivo activity has been demonstrated in mouse models, where it conferred resistance to high-fat diet-induced obesity [Patent: WO2016006548A1], the current study did not investigate its

effects on skin conditions or AhR-mediated pathways in vivo. Future studies are needed to assess whether FG1's observed effects on AhR signaling and artemin expression translate to therapeutic benefits in preclinical models of atopic dermatitis. Additionally, given AhR's abundant expression in epidermal keratinocytes, topical application of FG1 might offer a promising therapeutic approach by achieving higher local concentrations while minimizing systemic exposure. The concentration of FG1 in traditional Zhenjiang aromatic vinegar suggests that relevant doses could be achieved through dietary sources (Yatmaz et al., 2017), but comprehensive bioavailability studies are necessary to confirm this. Further research is also needed to comprehensively profile FG1 content across different vinegar-producing regions and microbial strains to better understand its natural distribution and production.

Finally, while FG1's antioxidant and Nrf2-activating properties suggest potential benefits in mitigating oxidative stress, this study did not directly examine the interplay between its antioxidant activity and AhR signaling in vivo. Exploring this connection further could provide a more comprehensive understanding of FG1's mechanisms and therapeutic relevance.

5. Conclusions

Our study demonstrates that FG1, a natural compound from traditional fermented vinegar, functions as a safe and potent AhR antagonist in epidermal cells. FG1 effectively suppressed FICZ-induced effects while exhibiting a favorable safety profile, making it a promising candidate for further toxicological evaluations in skin conditions where AhR signaling contributes to pathogenesis. The concentration of FG1 in traditional Zhenjiang aromatic vinegar suggests that relevant doses could be achieved through dietary sources (Yatmaz et al., 2017). Future research should focus on quantifying FG1 intake from typical vinegar consumption and assessing its bioavailability, as well as evaluating its potential as a topical agent to achieve higher local concentrations. These studies would provide critical insights into FG1's safety and efficacy as a modulator of AhR signaling.

CRediT authorship contribution statement

Kosuke Kato: Writing – original draft, Investigation, Formal analysis. **Miki Akamatsu:** Writing – original draft, Investigation, Formal analysis. **Saya Kakimaru:** Investigation. **Mayuko Koreishi:** Investigation. **Masahiro Takagi:** Writing – review & editing, Supervision, Conceptualization. **Masahiro Miyashita:** Supervision. **Yoshiyuki Murata:** Supervision, Conceptualization. **Yoshimasa Nakamura:** Writing – review & editing, Writing – original draft, Supervision, Conceptualization. **Ayano Satoh:** Writing – review & editing, Writing – original draft, Visualization, Methodology, Investigation, Formal analysis, Conceptualization. **Yoshio Tsujino:** Writing – review & editing, Supervision, Funding acquisition, Conceptualization.

Statement of informed consent

There are no human subjects in this article and informed consent is not applicable.

Declaration of Generative AI and AI-assisted technologies in the writing process

Statement: During the preparation of this manuscript, the authors used Claude 3.5 Sonnet for proofreading. The authors reviewed and edited all AI-assisted content and take full responsibility for the published work.

Funding

This work was supported by the Okayama Prefecture (Tokuden, A.S.) and by MEXT/JSPS KAKENHI (grant numbers 17H03818, 20H02933, and 23H02161 (Y.N.) and 18K06133 and 21H05028 (A.S.)).

The funding source(s) had no involvement in study design; in the collection, analysis and interpretation of data; and in the decision to submit the article for publication.

Declaration of competing interest

The authors declare that they have no known competing financial interests or personal relationships that could have appeared to influence the work reported in this paper.

Acknowledgements

We are grateful to all the members of the Organelle Laboratory (Okayama University) for their assistance and comments.

Appendix A. Supplementary data

Supplementary data to this article can be found online at https://doi.org/10.1016/j.fct.2025.115301.

Data availability

No data was used for the research described in the article.

References

Adachi, J., Mori, Y., Matsui, S., Takigami, H., Fujino, J., Kitagawa, H., Miller 3rd, C.A., Kato, T., Saeki, K., Matsuda, T., 2001. Indirubin and indigo are potent aryl hydrocarbon receptor ligands present in human urine. J. Biol. Chem. 276 (34), 31475–31478. https://doi.org/10.1074/jbc.C100238200.

Aggarwal, B.B., Ichikawa, H., 2005. Molecular targets and anticancer potential of indole-3-carbinol and its derivatives. Cell Cycle 4 (9), 1201–1215. https://doi.org/10.4161/cc.4.9.1993.

Aghababaei, F., Hadidi, M., . Recent Afvances in Potential Health Benefits of Quercetin. Pharmaceuticals 16 (7), 1020. https://doi.org/10.3390/ph16071020.

Bak, S.M., Iida, M., Soshilov, A.A., Denison, M.S., Iwata, H., Kim, E.Y., 2017. Auto-induction mechanism of aryl hydrocarbon receptor 2 (AHR2) gene by TCDD-activated AHR1 and AHR2 in the red seabream (Pagrus major). Arch. Toxicol. 91 (1), 301–312. https://doi.org/10.1007/s00204-016-1732-9.

Boitano, A.E., Wang, J., Romeo, R., Bouchez, L.C., Parker, A.E., Sutton, S.E., Walker, J.R., Flaveny, C.A., Perdew, G.H., Denison, M.S., Schultz, P.G., Cooke, M.P., 2010. Aryl hydrocarbon receptor antagonists promote the expansion of human hematopoietic stem cells. Science 329 (5997), 1345–1348. https://doi.org/10.1126/science.1191536.

Casper, R.F., Quesne, M., Rogers, I.M., Shirota, T., Jolivet, A., Milgrom, E., Savouret, J.F., 1999. Resveratrol has antagonist activity on the aryl hydrocarbon receptor: implications for prevention of dioxin toxicity. Mol. Pharmacol. 56 (4), 784–790.

Cheng, J., Wang, S., Lv, S.Q., Song, Y., Guo, N.H., 2023. Resveratrol inhibits AhR/Notch axis and reverses Th17/Treg imbalance in purpura by activating Foxp3. Toxicol. Res. 12 (3), 381–391. https://doi.org/10.1093/toxres/tfad021.

Ciumărnean, L., Milaciu, M.V., Runcan, O., Vesa, S.C., Răchişan, A.L., Negrean, V., Perné, M.G., Donca, V.I., Alexescu, T.G., Para, I., Dogaru, G., 2020. The effects of flavonoids in cardiovascular diseases. Molecules 25 (18), 4320. https://doi.org/10.3390/molecules25184320.

Dickschat, J.S., 2017. Fungal volatiles - a survey from edible mushrooms to moulds. Nat. Prod. Rep. 34 (3), 310–328. https://doi.org/10.1039/c7np00003k.

Dou, H., Duan, Y., Zhang, X., Yu, Q., Di, Q., Song, Y., Li, P., Gong, Y., 2019. Aryl hydrocarbon receptor (AhR) regulates adipocyte differentiation by assembling CRL4B ubiquitin ligase to target PPARγ for proteasomal degradation. J. Biol. Chem. 294 (48), 18504–18515. https://doi.org/10.1074/jbc.RA119.009282.

Eberhardt, J., Santos-Martins, D., Tillack, A.F., Forli, S., 2021. AutoDock Vina 1.2.0: new docking methods, expanded force field, and Python bindings. J. Chem. Inf. Model. 61 (8), 3891–3898. https://doi.org/10.1021/acs.jcim.1c00203.

Edamitsu, T., Taguchi, K., Kobayashi, E.H., Okuyama, R., Yamamoto, M., 2019. Aryl hydrocarbon receptor directly regulates *Artemin* gene expression. Mol. Cell Biol. 39 (20), e00190. https://doi.org/10.1128/MCB.00190-19, 19.

Gong, D., Lei, J., He, X., Hao, J., Zhang, F., Huang, X., Gu, W., Yang, X., Yu, J., 2024. Keys to the switch of fat burning: stimuli that trigger the uncoupling protein 1 (UCP1) activation in adipose tissue. Lipids Health Dis. 23 (1), 322. https://doi.org/10.1186/s12944-024-02300-z.

Goya-Jorge, E., Jorge Rodríguez, M.E., Sylla-Iyarreta Veitía, M., Giner, R.M., 2021. Plant occurring flavonoids as modulators of the aryl hydrocarbon receptor. Molecules 26 (8), 2315. https://doi.org/10.3390/molecules26082315.

Haddad, J.J., Olver, R.E., Land, S.C., 2000. Antioxidant/pro-oxidant equilibrium regulates HIF-1alpha and NF-kappa B redox sensitivity. Evidence for inhibition by

glutathione oxidation in alveolar epithelial cells. J. Biol. Chem. 275 (28), 21130–21139. https://doi.org/10.1074/jbc.M000737200.
Hidaka, T., Ogawa, E., Kobayashi, E.H., Suzuki, T., Funayama, R., Nagashima, T., Fujimura, T., Aiba, S., Nakayama, K., Okuyama, R., Yamamoto, M., 2017. The aryl hydrocarbon receptor AhR links atopic dermatitis and air pollution via induction of the neurotrophic factor artemin. Nat. Immunol. 18 (1), 64–73. https://doi.org/10.1038/ni.3614.
Huang, W., Zhong, Y., Gao, B., Zheng, B., Liu, Y., 2023. Nrf2-mediated therapeutic effects of dietary flavones in different diseases. Front. Pharmacol. 14, 1240433. https://doi.org/10.3389/fphar.2023.1240433.
Hubbard, T.D., Murray, I.A., Perdew, G.H., 2015. Indole and tryptophan metabolism: endogenous and dietary routes to Ah receptor activation. Drug Metabol. Dispos. 43 (10), 1522–1535. https://doi.org/10.1124/dmd.115.064246.
Jin, U.H., Park, H., Li, X., Davidson, L.A., Allred, C., Patil, B., Jayaprakasha, G., Orr, A.A., Mao, L., Chapkin, R.S., Jayaraman, A., Tamamis, P., Safe, S., 2018. Structure-dependent modulation of aryl hydrocarbon receptor-mediated activities by flavonoids. Toxicol. Sci. 164 (1), 205–217. https://doi.org/10.1093/toxsci/kfy075.
Kaushal, N., Singh, M., Sangwan, R.S., 2022. Flavonoids: food associations, therapeutic mechanisms, metabolism and nanoformulations. Food Res. Int. 157, 111442. https://doi.org/10.1016/j.foodres.2022.111442.
Koshino, H., Yoshihara, T., Okuno, M., Sakamura, S., Tajimi, A., Shimanuki, T., 1992. Gamahonolides A, B, and gamahorin, novel antifungal compounds from stromata of Epichloe typhina on Phleum pratense. Biosci. Biotechnol. Biochem. 56 (7), 1096–1099. https://doi.org/10.1271/bbb.56.1096.
Krieger, E., Vriend, G., 2014. YASARA View - molecular graphics for all devices - from smartphones to workstations. Bioinformatics 30 (20), 2981–2982. https://doi.org/10.1093/bioinformatics/btu426.
Kyunai, Y.M., Sakamoto, M., Koreishi, M., Tsujino, Y., Satoh, A., 2023. Fucosyltransferase 8 (FUT8) and core fucose expression in oxidative stress response. PLoS One 18 (2), e0281516. https://doi.org/10.1371/journal.pone.0281516.
Liu, Y., Myojin, T., Li, K., Kurita, A., Seto, M., Motoyama, A., Liu, X., Satoh, A., Munemasa, S., Murata, Y., Nakamura, T., Nakamura, Y., 2022. A major intestinal catabolite of quercetin glycosides, 3-hydroxyphenylacetic acid, protects the hepatocytes from the acetaldehyde-induced cytotoxicity through the enhancement of the total aldehyde dehydrogenase activity. Int. J. Mol. Sci. 23 (3), 1762. https://doi.org/10.3390/ijms23031762.
Luo, Z., Tian, M., Yang, G., Tan, Q., Chen, Y., Li, G., Zhang, Q., Li, Y., Wan, P., Wu, J., 2022. Hypoxia signaling in human health and diseases: implications and prospects for therapeutics. Signal Transduct. Targeted Ther. 7 (1), 218. https://doi.org/10.1038/s41392-022-01080-1.
Matsuda, H., Watanabe, N., Geba, G.P., Sperl, J., Tsudzuki, M., Hiroi, J., Matsumoto, M., Ushio, H., Saito, S., Askenase, P.W., Ra, C., 1997. Development of atopic dermatitis-like skin lesion with IgE hyperproduction in NC/Nga mice. Int. Immunol. 9 (3), 461–466. https://doi.org/10.1093/intimm/9.3.461.
Mimura, J., Ema, M., Sogawa, K., Fujii-Kuriyama, Y., 1999. Identification of a novel mechanism of regulation of Ah (dioxin) receptor function. Gene Dev. 13 (1), 20–25. https://doi.org/10.1101/gad.13.1.20.
Mo, Y., Lu, Z., Wang, L., Ji, C., Zou, C., Liu, X., 2020. The aryl hydrocarbon receptor in chronic kidney disease: friend or foe? Front. Cell Dev. Biol. 8, 589752. https://doi.org/10.3389/fcell.2020.589752.
Novotna, A., Pavek, P., Dvorak, Z., 2011. Novel stably transfected gene reporter human hepatoma cell line for assessment of aryl hydrocarbon receptor transcriptional activity: construction and characterization. Environ. Sci. Technol. 45 (23), 10133–10139. https://doi.org/10.1021/es2029334.
Rannug, A., Rannug, U., 2018. The tryptophan derivative 6-formylindolo[3,2-*b*] carbazole, FICZ, a dynamic mediator of endogenous aryl hydrocarbon receptor signaling, balances cell growth and differentiation. Crit. Rev. Toxicol. 48 (7), 555–574. https://doi.org/10.1080/10408444.2018.1493086.
Revel, A., Raanani, H., Younglai, E., Xu, J., Rogers, I., Han, R., Savouret, J.F., Casper, R. F., 2003. Resveratrol, a natural aryl hydrocarbon receptor antagonist, protects lung from DNA damage and apoptosis caused by benzo[a]pyrene. J. Appl. Toxicol. 23 (4), 255–261. https://doi.org/10.1002/jat.916.
Sato, H., Kato, K., Koreishi, M., Nakamura, Y., Tsujino, Y., Satoh, A., 2024. Aromatic oil from lavender as an atopic dermatitis suppressant. PLoS One 19 (1), e0296408. https://doi.org/10.1371/journal.pone.0296408.
Satsu, H., Yoshida, K., Mikubo, A., Ogiwara, H., Inakuma, T., Shimizu, M., 2015. Establishment of a stable aryl hydrocarbon receptor-responsive HepG2 cell line. Cytotechnology 67 (4), 621–632. https://doi.org/10.1007/s10616-014-9711-6.
Song, J., Clagett-Dame, M., Peterson, R.E., Hahn, M.E., Westler, W.M., Sicinski, R.R., DeLuca, H.F., 2002. A ligand for the aryl hydrocarbon receptor isolated from lung. Proc. Natl. Acad. Sci. USA 99 (23), 14694–14699. https://doi.org/10.1073/pnas.232562899.
Tabei, Y., Murotomi, K., Umeno, A., Horie, M., Tsujino, Y., Masutani, B., Yoshida, Y., Nakajima, Y., 2017. Antioxidant properties of 5-hydroxy-4-phenyl-butenolide via activation of Nrf2/ARE signaling pathway. Food Chem. Toxicol. 107 (Part A), 129–137. https://doi.org/10.1016/j.fct.2017.06.039.
Torti, M.F., Giovannoni, F., Quintana, F.J., García, C.C., 2021. The aryl hydrocarbon receptor as a modulator of anti-viral immunity. Front. Immunol. 12, 624293. https://doi.org/10.3389/fimmu.2021.624293.
Trott, O., Olson, A.J., 2010. AutoDock Vina: improving the speed and accuracy of docking with a new scoring function, efficient optimization, and multithreading. J. Comput. Chem. 31 (2), 455–461. https://doi.org/10.1002/jcc.21334.
Tsujino, Y., 2017. A new agonist for peroxisome proliferation-activated receptor γ (PPARγ), Fraglide-1 from Zhenjiang fragrant vinegar: screening and characterization based on cell culture experiments. J. Oleo Sci. 66 (6), 615–622. https://doi.org/10.5650/jos.ess16253.
Uchi, H., Yasumatsu, M., Morino-Koga, S., Mitoma, C., Furue, M., 2017. Inhibition of aryl hydrocarbon receptor signaling and induction of NRF2-mediated antioxidant activity by cinnamaldehyde in human keratinocytes. J. Dermatol. Sci. 85 (1), 36–43. https://doi.org/10.1016/j.jdermsci.2016.10.003.
Yatmaz, A.H., Kinoshita, T., Miyazato, A., Takagi, M., Tsujino, Y., Beppu, F., Gotoh, N., 2017. Quantification of Fraglide-1, a new functional ingredient, in vinegars. J. Oleo Sci. 66 (12), 1381–1386. https://doi.org/10.5650/jos.ess17147.
Zhang, X., Li, X., Fang, H., Guo, F., Li, F., Chen, A., Huang, S., 2019. Flavonoids as inducers of white adipose tissue browning and thermogenesis: signalling pathways and molecular triggers. Nutr. Metabol. 16, 47. https://doi.org/10.1186/s12986-019-0370-7.